Research Square

Preprints are preliminary reports that have not undergone peer review.
They should not be considered conclusive, used to inform clinical practice,
or referenced by the media as validated information.

Exosomal Carboxypeptidase E (CPE) and CPE-shRNA Loaded Exosomes Control Growth and Invasion of Recipient Hepatocellular Carcinoma Cells

Sangeetha Hareendran
National Institutes of Health
Bassam Albraidy
National Institutes of Health
Xuyu Yang
National Institutes of Health
Aiyi Liu
National Institutes of Health
Anne Breggia
Maine Medical Center Research Institute
Clark C Chen
University of Minnesota Medical School Twin Cities
Y. Peng Loh (lohp@mail.nih.gov)
National Institutes of Health https://orcid.org/0000-0002-5404-723X

Research Article

Keywords: Carboxypeptidase E, cancer proliferation, cancer biomarker, exosomes, hepatocellular carcinoma, metastasis, cancer therapy

Posted Date: March 24th, 2021

DOI: https://doi.org/10.21203/rs.3.rs-335388/v1

License: This work is licensed under a Creative Commons Attribution 4.0 International License.
Read Full License

Abstract

Background: Exosomes from cancer cells promote tumor growth and metastasis through intercellular communication. However, the exosomal bioactive molecules involved and the mechanism of action remain elusive. Carboxypeptidase E (CPE) is known to drive tumor progression in different cancers, including hepatocellular carcinoma (HCC), which is associated with high mortality rate. Here, we investigated if CPE is present within cancer cell exosomes and contributes to the molecular pathogenesis of HCC and other cancers by regulating tumor growth and invasion.

Methods: Exosomes isolated from the culture media of cancer cells or human serum were analyzed for *CPE* mRNA and protein using quantitative PCR/ RT-PCR and western blot respectively. Low-metastatic HCC97L cells were incubated with exosomes derived from high-metastatic HCC97H cells. In other experiments, HCC97H cells were incubated with CPE-shRNA loaded exosomes isolated from HEK293T cells. The recipient HCC cells were assessed for proliferation and invasion using MTT cell proliferation, colony formation and matrigel invasion assays.

Results: *CPE* mRNA and protein were found to be packaged within exosomes released from cancer cells. We observed elevated *CPE* mRNA levels in secreted exosomes from high versus low-malignant cells, from various cancer types including HCC, breast cancer and glioblastoma. In a pilot study, significantly higher *CPE* copy numbers were found in serum exosomes from cancer patients compared to healthy donors, suggesting that exosomal CPE mRNA could be a potential diagnostic biomarker. Low-malignant HCC97L cells treated with exosomes derived from HCC97H cells, displayed enhanced proliferation and invasion; however exosomes from HCC97H cells pre-treated with CPE-shRNA failed to promote proliferation. When HEK293T exosomes loaded with CPE-shRNA, were incubated with HCC97H cells, expression of CPE, Cyclin D1, a cell-cycle regulatory protein and c-MYC, a proto-oncogene, were suppressed, resulting in diminished proliferation of HCC97H cells.

Conclusions: Our results identified CPE as a bioactive molecule in exosomes driving the growth and invasion of low-malignant HCC cells, and showed that CPE-shRNA loaded exosomes can inhibit malignant tumor cell proliferation *via* Cyclin D1 and c-MYC suppression. Thus, CPE is a key player in exosome transmission of tumorigenesis, and exosome-based delivery of CPE-shRNA offers a potential treatment for tumor progression.

Background

Metastatic colonization of tumor cells to distant organs and drug resistance are the biggest challenges to cancer therapy today [1]. One such metastatic cancer, hepatocellular carcinoma (HCC) is the primary malignancy which affects the liver and is the ninth leading cause of cancer deaths in the United States, with average survival rate of 6-20 months [2]. Liver transplantation and surgical resection are the two most effective treatment options available for patients, besides local therapies such as ablation or trans-arterial embolization and systemic therapy with multikinase inhibitor Sorafenib [3]. Despite all these

accessible interventions, the mortality rates of patients remain high because HCC is often diagnosed at advanced stages and tumor recurrence poses a major challenge [4]. Therefore, shifting focus to better understand the molecular pathogenesis of HCC, identification of prognostic prediction biomarkers and novel targets for intervention are of high priority.

Exosomes, which are nano-sized extracellular vesicles (30-140nm in diameter) secreted by most cells, facilitate critical intercellular communication by way of transferring bioactive molecules. Importantly, exosomes derived from tumor cells have distinct composition to those released from healthy cells [5]. Tumor-derived exosomes are known to promote tumorigenesis, metastasis and modulation of tumor microenvironment [6-8]. A recent report showed that exosomes released from highly malignant hepatocellular carcinoma (HCC) cells could increase tumorigenic and migratory functions of low-malignant HCC cells by inducing EMT (epithelial- mesenchymal transition) *via* MAPK/ERK pathway [9]. Primary HCC-derived exosomes support metastases by enhancing SMAD3 signaling in circulating tumor cells to promote their adhesion [10]. Additionally, exosomes can serve as a safe delivery system for siRNA/shRNA related interventions [11]. Using orthotopic pancreatic cancer mouse models, it was demonstrated that exosomes carrying *KRAS* specific siRNA could suppress tumor growth, inhibit metastasis and improve overall survival [12]. It remains to be determined what exosomal factors induce tumor growth and metastasis in HCC and other cancers, and whether exosomes can be exploited for targeted cancer therapy.

Carboxypeptidase E (CPE) is an exopeptidase, initially discovered as a prohormone processing enzyme [13, 14]. Subsequently, non-enzymatic functions of CPE as a sorting receptor for prohormones and a trophic factor in mediating cell survival have been reported [15-17]. In cancer, aberrant upregulation of CPE is found in endocrine tumors (pituitary adenomas) [18] as well as non-endocrine tumors (cervical, colorectal, ovarian and pancreatic cancer, HCC and glioma) [19-23]. CPE has varying effects on tumor growth and metastasis depending on the type of tumor. For example, CPE promotes cell proliferation and migration in osteosarcoma, colorectal and pancreatic cancer cell lines, while in glioma and fibrosarcoma cells, it exerts an anti-migratory /anti-invasion effect [19, 21, 24-26]. Besides the full length wild-type CPE (WT-CPE), a 40kDa splice variant of CPE (CPE-ΔN) has been cloned and shown to promote tumor cell proliferation and invasion, by a distinct mechanism [27, 28]. This 40kDa CPE-ΔN variant is a N-terminal truncated form of the CPE protein and is translocated into the nucleus to induce expression of metastasis associated genes [28]. Given the multi- faceted role of CPE in tumorigenesis, we investigated if CPE could play a critical role in the exosomal transmission of tumorigenesis.

In this study, we determined 1) if *CPE* mRNA and protein are present within exosomes secreted from cancer cells, and if exosomal CPE can confer growth and metastasis of cancer cells; and 2) whether CPE-shRNA loaded exosomes could be taken up by malignant cancer cells to inhibit tumor growth as a potential therapeutic strategy. We demonstrated the presence of *CPE* mRNA within exosomes isolated from various cancer cell lines differing in malignant potential, and in serum-derived exosomes from cancer patients. We found that *CPE* mRNA is enriched in exosomes released from highly malignant cells of different cancer origin. Moreover, our pilot study using patient-derived sera exosomes showed that *CPE*

mRNA in circulating exosomes could be developed as a diagnostic cancer biomarker. We characterized the *CPE* mRNA and protein within exosomes from HCC cells, and showed that down-regulation of CPE in the parental HCC97H (high-malignant) cells prior to exosome isolation prevented the exosomal transfer of malignant properties from HCC97H to HCC97L (low-malignant) cells. We also tested whether the exosomal route could be used to deliver CPE-shRNA to target HCC cells to inhibit proliferation and determined the possible mechanism involved. Notably, the exosomes loaded with CPE-shRNA, inhibited the growth of recipient HCC cells by suppressing Cyclin-D1 and c-MYC expression. These findings indicate that exosomal CPE and modified exosomes enclosing CPE specific shRNA can modulate the malignant properties of cancer cells.

Methods

Cell culture

Human cancer cell lines HCC97H, HCC97L (liver cancer); MDA-MD-231, MCF-7 (breast cancer); AsPC-1, BxPC-3 (pancreatic cancer), HT-29, SW480 (colorectal cancer), DU145, LNCaP (prostate cancer) and LN-18, UM18 (glioblastoma) exhibiting either high or low-malignant potential respectively, and highly malignant CAOV3 cells (ovarian cancer) were cultured in DMEM medium supplemented with 10% fetal bovine serum at 37°C in a humidified 5% CO_2 incubator. The various cancer cell lines were seeded at approximately equal numbers in the culture dish and maintained at similar conditions such as volume of growth media and incubation time. All cell lines, except HCC cells, were obtained from ATCC (Manassas, Virginia). Human HCC cell lines with low and high-malignant potential, MHCC97L and MHCC97H (referred in this study as HCC97L and HCC97H) respectively derived from the same parental cell line, were obtained from Liver Cancer Institute, Fudan University (Shanghai, China).

Isolation of exosomes

When cells seeded in a 60mm dish reached 75% confluency (~$2.5x10^6$ cells), the supernatant media was collected and pre-cleared of cell debris by centrifugation at 2500rpm for 10min at 4 ˚C. Exosomes were isolated from the pre-cleared supernatant culture media of cells using ExoQuick TC reagent (System Biosciences, EXOTC50A-1) according to manufacturer's instructions. Briefly, 1ml of reagent was added per 5ml of culture media and incubated at 4˚C for at least 12 h . Exosomes present in the incubated media were then pelleted down by centrifugation at 1500g for 30min and resuspended in either 50µl of PBS or TRI reagent for RNA isolation or in RIPA protein lysis buffer for western blot and stored in -80˚C until further use. Serum exosomes were isolated from 250µl serum using ExoCap composite kit (MBL International, Woburn, MA) per instruction manual, which is based on an antibody coupled magnetic capture bead-based procedure. The kit contains mixture of CD9, CD63, CD81 and EpCAM capture beads. This step was followed by purification of exosomal RNA using ExoCap Nucleic acid elution buffer (MBL International, MEX-E kit) according to the kit protocol.

NanoSight analysis

The nanoparticle tracking analysis (NTA) was performed to determine size distribution and concentration of exosomes using NanoSight LM10 instrument (Malvern), equipped with a 405 nm LM12 module and EM-CCD camera (DL-658-OEM-630, Andor) and NTAv3.1 software (Malvern Panalytical, Malvern, U.K). Two microlitres of exosomes was diluted with 500µl of PBS before analysis. The dilution factor was accounted to obtain the final exosome concentrations. Results are displayed as a graph with size (nm) vs concentration (particles/ml) measurements and a scatter plot with size (nm) vs intensity (a.u).

RT-PCR

cDNA was synthesized from 3-6 µg of RNA from exosomes using sensiFAST cDNA synthesis kit (BIOLINE Meridian Bioscience, BIO-65053) based on manufacturer's instructions. CPE transcript was amplified using SeqAMP DNA polymerase (Clonetech, catalog no: 638509) and different primer sets as indicated in the corresponding figure. Primer sequences are given in additional file 2: Table S1. PCR cycle consisted of an initial 'hot start' at 94°C for 3min followed by 35 cycles of amplification (94°C 30 sec, 60°C 30 sec, 72°C 30sec) with a final extension step of 72°C for 5 min. PCR products were analyzed on 1.8% agarose gels.

Quantitative real-time PCR

Exosomal RNA was purified from supernatant media of cells using SeraMir kits (System Biosciences, RA800A) or TRIzol reagent (Sigma), and from serum using ExoCap composite kits. The first-strand cDNA was synthesized with 0.1µg of total RNA using SensiFast cDNA Synthesis kit. qRT-PCR was performed using SYBR Green PCR Matrix Mix (Applied BioSystem, #4367659) in an ABI PRISM 7900 Sequence Detector (Applied Biosystems) with cycling conditions as: 95°C for 5min, followed by 40 amplification cycles of denaturation 95°C for 15sec, annealing 60°C for 60sec, and extension 72°C for 30 sec and final extension at 72°C for 10min. Standard curve method using CPE 5'-DNA fragment of known concentration was used to perform quantitation of *CPE* mRNA copy numbers in exosomes using CPE 5' primer set. All samples for copy number determination including the standard curve were run together in a 384-well PCR plate. The 2−ΔΔCt method was used to calculate the relative fold difference of mRNA expression of *CPE, Cyclin D1* and *c-MYC* in HCC97L and HCC97H cells. 18s rRNA was used for data normalization. Primer sequences used are listed in additional file 2: Table S1. All qRT-PCR assays were run in triplicate.

Western blot

Exosome/ cellular protein lysates were prepared using RIPA lysis and extraction buffer (Thermo Scientific, #89901) supplemented with Halt Protease inhibitor cocktail (Thermo Scientific, #87786). Forty-five µg of exosomal protein or 25 µg of cellular protein was loaded per lane of the SDS-PAGE gel, and western blot was performed as described previously [26]. For analysis of secreted WT-CPE, supernatant media of cells were concentrated using Amicon Ultra 10k MWCO centrifugal filter (Millipore Sigma). Monoclonal antibody against CPE (#610758, 1:2000 dilution) was purchased from BD Biosciences, and primary antibodies to TSG101 (Tumor susceptibility gene 101, ab612696, 1:500 dilution) and CD63 (ab68418,

1:1000 dilution) were from Abcam (Cambridge, MA). Cyclin D1 (#92G2, 1:500) antibody was from Cell Signaling Technology and β-tubulin (#T5168, 1:2000) was procured from Sigma- Aldrich.

In vitro exosome transfer experiments

To perform exosome transfer experiments using HCC97H-derived exosomes, HCC97H cells were seeded in a 60mm dish and transfected with either 25nM CPE-shRNA or control shRNA plasmids (Santa Cruz Biotechnology Inc, Cat#sc-45378-SH, sc-108060) using Lipofectamine 2000 reagent (Thermo Scientific). Forty-eight hours later, the supernatant media of the transfected cells were collected, and exosomes were isolated. Exosomes were also isolated from culture media of untransfected HCC97H cells (ExoHCCH) for some experiments. After dissolving the exosome pellet in 50µl of PBS, the exosomal protein was estimated using protein assay (Bio-Rad, Cat#500-0006). HCC97L cells seeded in a 6-well plate were treated with 75µg of exosomal protein/ well for 48 h, after which the cells were harvested, and seeded for MTT and cell invasion assays. Based on the NanoSight analyses of ExoHCCH, ExoHCCH-CPE-shRNA and ExoHCCH-CTRL-shRNA, the number of particles added was quantitated to be approximately equal to 55-70x10^{10} particles/ well.

For experiments targeting HCC97H with CPE-shRNA loaded exosomes, HEK293T (Human embryonic kidney expressing mutant allele of SV40 T antigen) cells were infected with adenovirus carrying either CPE-shRNA-GFP (GFP, green fluorescent protein) or control-shRNA-GFP (Vector Biolabs) at MOI 25 for 48-72 h. After 5-6 hours of infection, the culture media was replaced to remove viral particles present in the infection media. Exosomes were isolated from the supernatant media of the infected cells, and the exosomal protein was estimated. To compare and standardize exosome loading, 25 µg of the exosomal protein (exoHEK) either exoHEK-CPE-shRNA or exoHEK-CTRL-shRNA, were used to treat HCC97H cells, seeded in 4-well chamber slides. 48 h later, the GFP fluorescence of the cells, which is an indirect measurement of shRNA loading and transfer *via* exosomes, was documented using a fluorescent microscope (Eclipse 80i, Nikon or Zeiss Wide-Field) and the GFP levels were quantitated using Image J software. The fold change difference in the GFP levels between ExoHEK-CPE-shRNA and ExoHEK-CTRL-shRNA treated HCC97H cells, if any, is determined. Subsequently, HCC97H cells seeded in a 30mm dish were treated with 100µg of ExoHEK-CPEshRNA. The amount of ExoHEK-CTRL-shRNA to be added was calculated based on the fold change difference in the GFP levels, determined by Image J software analysis of fluorescent images, performed in the prior standardization step, such that the GFP levels between the ExoHEK-CPE-shRNA and ExoHEK-CTRL-shRNA treatment groups are comparable. After 48 h, the cells were seeded for MTT and colony formation assays.

Statistical analysis

Data represents mean±SD (standard deviation) or mean±SE (standard error) of independent experiments (N), performed in triplicate (n=3) or as stated in the figure legend. Statistical significance was determined using Student's t-test and p values are denoted as*$p < 0.05$, **$p < 0.01$, ***$p < 0.001$. Box plot and Shapiro-Wilk normality test were used to examine the distribution of *CPE* copy numbers in human sera exosomes.

Logistic regression and receiver operating characteristics (ROC) curve analysis were performed to investigate the association of cancers with *CPE* copy number in sera derived exosomes.

Results

Presence of CPE in exosomes derived from HCC cells

Particle analyses revealed that exosomes derived from HCC cells with high and low-malignant potential, were approximately 100nm in diameter as depicted in the representative graphs in Fig. 1 (a-b). These vesicles were characterized by the presence of exosome specific markers CD63 and TSG101 along with the presence of CPE (Fig. 1e). We did not find any correlation between the size and number of exosomes released, and the malignant potential of the HCC cells (Fig. 1a-b). This finding was confirmed using exosomes isolated by a different procedure (iZON columns), as described in additional file 2: Supplemental experimental procedures, Table S3 and additional file 1: Fig. S1. A similar lack of correlation between size/ number and malignancy was observed for exosomes derived from different cancer cell lines (breast, pancreatic, colon or prostate cancers) (additional file 1: Table S2).

To determine if *CPE* mRNA and its splice variant, CPE-ΔN, are present within exosomes derived from three different cancer cell lines, we used a specific primer set F134/ R667 which flanks the region of deletion in exon1 to differentiate *CPE-ΔN* mRNA sequence in addition to primers flanking rest of the CPE mRNA. Primer sequences used are given in additional file 2: Table S1. The position of the deletion in CPE-ΔN and the primer sets used for PCR are shown in Fig. 1c. As shown in Fig. 1d, the amplified PCR region in exosomes derived from CAOV3 (ovarian cancer), HCC97H (liver cancer) and MDA-MB-231 (breast cancer) cell lines corresponds to WT-CPE gene segments, and not CPE-ΔN. Using overlapping primer sets we could amplify close to 1kb from the 5' end to the middle portion of *CPE* mRNA, while parts of 3' region were missing, as shown in additional file 1: Fig. S2. Although we were unable to amplify the full-length mRNA of *CPE*, the contiguous portion of the mRNA that we amplified, in fact, encodes the entire coding sequence of *CPE* mRNA. For analysis of CPE protein, western blot of exosomes derived from HCC97H and HCC97L was carried out (Fig. 1e). A band of ~50kDa which corresponds to the size of WT-CPE (~50-53kDa), but not 40kDa CPE-ΔN band was detected. Our results indicate that HCC exosomes contain both *CPE* mRNA and protein. Other exosomes from ovarian and breast cancer cells also contain *CPE* mRNA and likely protein as well.

Exosomes isolated from highly malignant cancer cells show elevated *CPE mRNA* levels

Elevated expression levels of CPE have been associated with malignancy in various types of cancer cell lines *in vitro* and patient tumors [19-22, 24, 25]. Based on our data suggesting that cancer cell exosomes contain CPE, we then determined if levels of *CPE* mRNA within exosomes released from cancer cells correlate with their malignancy. Fig. 2 (a-e) shows that significantly higher *CPE* mRNA copy numbers are present in exosomes released from highly malignant cancer cells compared to those released from cancer cell lines with low malignancy, across various types of cancer such as HCC, glioblastoma, prostate

cancer, colon cancer and pancreatic cancer. These data indicate that exosomes with elevated levels of *CPE* mRNA copy numbers are associated with the high-malignant phenotype.

Serum exosomes from cancer patients have higher CPE copy numbers than healthy controls

Given that elevated *CPE* mRNA level is correlated with malignancy in cancer cell lines, we have examined the *CPE* mRNA copy number in human sera exosomes derived from patients with different types of cancer and healthy controls (see additional file 2: Table S4 for subject details) in a pilot study. The *CPE* copy number in serum-derived exosomes are summarized using mean (standard deviation, SD) and median (interquartile range, IQR). For the cancer cases, the mean is 648.07 (SD=1122.41) and the median is 365.30 (IQR= 525.30-251.21=274.09); for the normal cases, the mean is 132.91 (SD=72.75) and the median is 115.20 (IQR=178.06-88.76=89.30). The Shapiro-Wilk normality test on the *CPE* copy number data in cancer cases showed significant departure from normality ($P<0.0001$). Therefore, the log10 transformed data, presented in Fig. 3a using box plots, are used for analysis. Logistic regression performed on the log10-transformed data showed that *CPE* copy number in sera exosomes is significantly associated with cancer (beta=6.21, $P=0.0004$); a 20% increase in copy number corresponds to 64% increase in the odds of developing cancer. The empirical receiver operating characteristics (ROC) curve (Fig. 3b) and its relatively large area under the curve (AUC= 0.88) corroborates the logistic regression analysis. The results indicate that higher *CPE* copy numbers are found in sera exosomes from cancer patients. However, an elaborate study with more patient samples is warranted to validate this finding.

Exosomes released from HCC97H cells enhance proliferation and invasion of recipient HCC97L cells in a CPE-dependent manner

As exosomes mediate cell-cell communication by transfer of cargo, we investigated if exosomal CPE taken up by recipient cells can modulate their proliferation and invasion. We found that incubation of HCC97L cells with HCC97H-derived exosomes increased their proliferation by ~36% in the MTT assay (Fig. 4a) and invasion through matrigel by 2-fold (Fig. 4d). However, downregulation of CPE by specific shRNA in HCC97H cells prior to exosome isolation abolished the effect of these exosomes on growth (Fig. 4b) and invasion of HCC97L cells (Fig. 4e). Moreover, these exosomes also down-regulated CPE expression levels in HCC97L cells, possibly by transfering CPE-shRNA to the target cells (Fig. 4c). These results indicate that exosomes isolated from HCC cells with high malignancy, when incubated with low-malignant HCC cells, can enhance their growth and metastatic properties, and that CPE plays an important role in this process.

Exosomes loaded with CPE-shRNA inhibit proliferation of highly malignant HCC cells

Previous reports have shown that injection of exosomes carrying *KRAS* siRNA could impede tumor growth and metastasis in pancreatic cancer mouse models [12]. Here, we tested if we could load HEK293T cell- derived exosomes with CPE-shRNA using adenovirus infection and then transfer the shRNA *via* the exosomes to target the proliferation of recipient HCC97H cells. Indeed, we detected

fluorescence signal of the GFP protein fused to the CPE-shRNA in the recipient HCC97H cells, after incubation with the exosomes isolated from HEK293T cells (ExoHEK) infected with adenovirus encoding CPE-shRNA-GFP (schematic of exosome loading and transfer is shown in Fig. 5a). These shRNA loaded ExoHEK were characterized by NanoSight analysis and visualized using TEM, as shown in Fig. 5b, additional file 1: Fig. S3 and additional file 2: Table S5. No viral particles were observed in the exosome preparation. Following treatment with ExoHEK-CPE-shRNA, a 4.74-fold reduction in *CPE* mRNA levels (Fig. 6a) and a 70% reduction of secreted CPE protein (Fig. 6b) were observed in the HCC97H cells, concomitant with a 3-fold decrease in cell proliferation at D7/8 (Fig. 6c, MTT assay) and a 5.3- fold reduction in the number of colonies formed (Fig. 6d-e). Furthermore, there was a down-regulation of expression of the cell cycle regulator, Cyclin D1 at the mRNA (Fig. 6f) and protein levels (Fig. 6g) in HCC97H cells treated with CPE-shRNA loaded exosomes, consistent with the decrease in proliferation. Importantly, expression of c-MYC, a transcription factor and proto-oncogene, was found to be significantly reduced in the ExoHEK-CPE-shRNA treated HCC97H cells (Fig. 6h). These results show that down-regulation of CPE through exosome-mediated shRNA delivery can inhibit proliferation of highly malignant liver cancer cells.

Discussion

Exosomes or extracellular vesicles are known to promote growth and metastasis of liver and other cancers, through intercellular communication, but their internal cargo driving these effects remain unclear. Liquid biopsy assays utilizing tumor exosomes, present in many biological fluids, are being developed to diagnose and predict prognosis of cancers such as melanoma, prostate cancer, glioblastoma and pancreatic cancer [29-32]. Serum levels of exosomal miRNAs such as miR-21, miR-141, miR-718 have been correlated with advanced stages of squamous cell carcinoma, prostate cancer and HCC recurrence after liver transplant, respectively [29, 33]. Elevated expression of CPE in tumors has been correlated with poor outcome in patients with cervical and pancreatic cancer, and hepatocellular carcinoma [20-22]. Furthermore, CPE has been shown to promote survival, growth and invasion of tumor cells [19, 21, 25, 26, 34]. We therefore investigated whether CPE is present within cancer cell exosomes and if so, does it play a pivotal role in promoting tumor cell proliferation and invasion in recipient cells. Indeed, we found *CPE* mRNA within the exosomes derived from liver, breast and ovarian cancer cells. *CPE-WT* mRNA, but not the *CPE-ΔN* variant was present within cancer cell exosomes. Interestingly, the contiguous portion of the mRNA (~1.2kb) that we detected encodes the entire coding region of *CPE*, with some of the noncoding 3' end missing. Full-length *CPE* in HCC and other cancer cells is ~2.4kb [28] and while it is possible that this 1.2kb transcript of *CPE* mRNA could be successfully translated to yield a functional protein, future studies will determine this. Within the exosomes derived from HCC97H and HCC97L cells, we found a ~50 kDa CPE protein approximating the size reported for WT-CPE. These data reveal that both *CPE* mRNA and protein are packaged inside cancer cell exosomes.

Consistent with reports that elevated CPE expression levels in tumors correlate with progression of the disease [19-22, 24, 25], we demonstrated that *CPE* mRNA copy numbers are significantly higher in exosomes isolated from highly malignant cancer cells compared to low-malignant cancer cell exosomes,

across different cancer types. This finding suggests that circulating exosomal CPE could potentially serve as a useful biomarker to detect cancer in patients. To this end, as a proof of concept, we showed that significantly high *CPE* mRNA copy numbers are present in sera-derived exosomes from patients with various types of cancer versus normal healthy controls. However, while the results are promising, this remains a pilot clinical study as the sample size is small, and extensive studies with more patients with different cancer types are necessary to develop the use of exosomal CPE as a clinical first screen biomarker for cancer.

Accumulating evidence suggest that transfer of exosomal cargo is linked to cellular communication within the tumor microenvironment and metastatic disease development. Exosomes from highly metastatic melanoma 'educate' bone marrow progenitors by elevating their MET receptor (hepatocyte growth factor receptor) expression, thereby facilitating primary tumor growth and metastasis [8]. Previous studies have shown that it is possible to transfer metastatic behavior of highly malignant cancer cells to those with low malignancy through exosomes [35]. Our study demonstrated that both proliferation and invasion of HCC97L cells were significantly increased by incubation with HCC97H exosomes. Most importantly, we showed that this phenocopying of malignant behavior in HCC cells *via* exosomes was dependent on CPE. Thus, our data indicate that the exosomal cargo, CPE, plays a key role in exosome-mediated cell-cell communication to promote liver cancer proliferation and invasion. As we found that elevated *CPE* mRNA levels in exosomes correlated with high malignancy in many other cancer cells including breast cancer, prostate cancer, pancreatic cancer, and glioblastoma, exosomal CPE could also likely promote proliferation and invasion of these cancer types. The mechanism by which exosome associated CPE transfers the malignant phenotype to recipient cells requires more investigation. However, our finding that exosome-based transfer of CPE-shRNA suppresses Cyclin D1 and c-MYC in recipient HCC97H cells suggests that exosomal *CPE* mRNA or protein exerts its effects through up-regulating these genes in recipient cells. Indeed, earlier reports have suggested that Cyclin D1 acts downstream of CPE in colorectal cancer and osteosarcoma cells, to promote proliferation of these cells [10, 24, 25].

Exosomes have been shown to act as vehicles to safely deliver cargo such as siRNA to brain and pancreas [12, 36]. We showed that CPE-shRNA transferred *via* exosomes to HCC97H cells can down-regulate their tumorigenic propensity, through suppression of Cyclin-D1 and c-MYC levels. In general, over-expression of Cyclin D1 is associated with tumor progression, chemotherapeutic resistance and metastasis [37, 38] while upregulation of c-MYC, a transcription factor that regulates proliferation and cell-cycle progression, is strongly correlated with poor prognosis in liver cancer patients, including metastasis [39]. p53 mutations, when combined with constitutive activation of c-MYC, can lead to DNA damage and induce liver tumorigenesis [40]. Our results highlight the potential of exosomes harboring CPE-shRNA to be developed as a therapeutic agent for treating HCC. Interestingly, treatment with exosomes carrying shRNA to target *KRAS* has suppressed tumor progression and enhanced survival in pancreatic cancer mouse models [12]. A similar strategy using CPE-shRNA loaded exosomes could also be applied to other tumors such as glioma, osteosarcoma, colorectal cancer and pancreatic cancer, where CPE plays a pro-tumorigenic role.

Conclusion

We have identified a new bioactive molecule in exosomes, CPE, that has the ability to transfer malignant phenotype from low to high-malignant HCC cells, suggesting that circulating exosomes carrying CPE may represent a novel mechanism for promoting tumor metastasis in the body. Furthermore, our data show that exosomes modified to carry CPE-shRNA could suppress tumor growth and be a potentially exciting new therapy for treating liver and other cancers, since CPE expression is upregulated in many cancer types. Our pilot clinical study suggests that *CPE* mRNA in circulating exosomes could be developed as a biomarker for diagnosing cancer. Future investigations will focus on translating our findings to pre-clinical models and advancing the potential clinical use of exosome-based delivery of CPE-shRNA in the treatment of different types of cancer.

Abbreviations

CPE Carboxypeptidase E

HCC Hepatocellular carcinoma

HEK Human embryonic kidney

TSG101 Tumor susceptibility gene 101

AUC Area under the curve

ROC Receiver operating characteristics

GFP Green fluorescent protein

NTA Nanoparticle tracking analysis

EMT Epithelial-Mesenchymal Transition

Declarations

Ethics Approval and Consent to participate

Serum samples from patients diagnosed with different types of cancers were obtained from Maine Medical Center BioBank, Portland, ME, which operates under an Institutional Review Board (IRB) approved protocol and is overseen by the MMCRI Office of Research Compliance (FWA00003993) and UCSD Medical Center, San Diego, CA (IRB 120345). Sera from healthy donors were obtained at the National Institutes of Health from The Blood Bank and under protocol 00-CH-0093, approved by IRB of the *Eunice Kennedy Shriver* National Institute of Child Health and Human Development, Bethesda, MD, USA. All serum samples were coded and unidentified. Consent to participate – not applicable.

Consent for publication

There are no details, images or videos relating to an individual person in the manuscript

Availability of supporting data

Data supporting the findings of this study are contained within the article and the additional supplemental files. All data discussed in the paper and all materials will be made available to readers upon request from the corresponding author.

Competing interests

The authors declare no competing financial interest.

Funding

This research was supported by the Intramural Research Program of the *Eunice Kennedy Shriver* National Institute of Child Health and Human Development (NICHD), National Institutes of Health and the National Cancer Institute, USA.

Author's contributions

YPL and XY designed the study. SH, BA, AL, AB, and CCC performed the experiments. YPL, SH, XY, AL analyzed data. YPL and SH wrote the manuscript. XY, AL, AB, and CCC reviewed the manuscript. All authors read and approved the final manuscript.

Acknowledgements

We thank Dr. Jennifer Clare Jones and Bryce Killingsworth (Center for Cancer Research, NCI) for their contributions towards NanoSight and NanoFACS analyses, and exosome isolation using iZON method; Louis Dye, Lynne Holtzclaw and Dr. Vincent Schram (NICHD Microscopy Core Facility) for their assistance in electron microscopy and Dr. Wei Zhang, Biostatistics & Bioinformatics Branch (NICHD) for help with statistical analysis. We thank Dr. Karel Pacak (NICHD) and the NIH blood bank for providing sera from healthy volunteers.

Author's information

Not applicable

References

1. Steeg PS. Targeting metastasis**.** Nat Rev Cancer. 2016; 16**:**201-218.
2. Balogh J, Victor D, 3rd, Asham EH, Burroughs SG, Boktour M, Saharia A, Li X, Ghobrial RM, Monsour HP, Jr. Hepatocellular carcinoma: a review**.** J Hepatocell Carcinoma. 2016; 3**:**41-53.

3. Waller LP, Deshpande V, Pyrsopoulos N. Hepatocellular carcinoma: A comprehensive review. World J Hepatol. 2015; 7:2648-2663.
4. Gomaa A, Waked I. Management of advanced hepatocellular carcinoma: review of current and potential therapies. Hepatoma Res. 2017; 3:112-122.
5. Sun W, Luo JD, Jiang H, Duan DD. Tumor exosomes: a double-edged sword in cancer therapy. Acta Pharmacol Sin. 2018; 39:534-541.
6. Hoshino A, Costa-Silva B, Shen TL, Rodrigues G, Hashimoto A, Tesic Mark M, Molina H, Kohsaka S, Di Giannatale A, Ceder S, et al. Tumour exosome integrins determine organotropic metastasis. Nature. 2015; 527:329-335.
7. Luga V, Wrana JL. Tumor-stroma interaction: Revealing fibroblast-secreted exosomes as potent regulators of Wnt-planar cell polarity signaling in cancer metastasis. Cancer Res. 2013; 73:6843-6847.
8. Peinado H, Aleckovic M, Lavotshkin S, Matei I, Costa-Silva B, Moreno-Bueno G, Hergueta-Redondo M, Williams C, Garcia-Santos G, Ghajar C, et al. Melanoma exosomes educate bone marrow progenitor cells toward a pro-metastatic phenotype through MET. Nat Med. 2012; 18:883-891.
9. Chen L, Guo P, He Y, Chen Z, Chen L, Luo Y, Qi L, Liu Y, Wu Q, Cui Y, et al. HCC-derived exosomes elicit HCC progression and recurrence by epithelial-mesenchymal transition through MAPK/ERK signalling pathway. Cell Death Dis. 2018; 9:513.
10. Fu Q, Zhang Q, Lou Y, Yang J, Nie G, Chen Q, Chen Y, Zhang J, Wang J, Wei T, et al. Primary tumor-derived exosomes facilitate metastasis by regulating adhesion of circulating tumor cells via SMAD3 in liver cancer. Oncogene. 2018; 37:6105-6118.
11. El-Andaloussi S, Lee Y, Lakhal-Littleton S, Li J, Seow Y, Gardiner C, Alvarez-Erviti L, Sargent IL, Wood MJ. Exosome-mediated delivery of siRNA in vitro and in vivo. Nat Protoc. 2012; 7:2112-2126.
12. Kamerkar S, LeBleu VS, Sugimoto H, Yang S, Ruivo CF, Melo SA, Lee JJ, Kalluri R. Exosomes facilitate therapeutic targeting of oncogenic KRAS in pancreatic cancer. Nature. 2017; 546:498-503.
13. Fricker LD, Snyder SH. Purification and characterization of enkephalin convertase, an enkephalin-synthesizing carboxypeptidase. J Biol Chem. 1983; 258:10950-10955.
14. Hook VY, Loh YP. Carboxypeptidase B-like converting enzyme activity in secretory granules of rat pituitary. Proc Natl Acad Sci U S A. 1984; 81:2776-2780.
15. Cheng Y, Cawley NX, Loh YP. Carboxypeptidase E/NFalpha1: a new neurotrophic factor against oxidative stress-induced apoptotic cell death mediated by ERK and PI3-K/AKT pathways. PLoS One. 2013; 8:e71578.
16. Cool DR, Normant E, Shen F, Chen HC, Pannell L, Zhang Y, Loh YP. Carboxypeptidase E is a regulated secretory pathway sorting receptor: genetic obliteration leads to endocrine disorders in Cpe(fat) mice. Cell. 1997; 88:73-83.
17. Dhanvantari S, Loh YP. Lipid raft association of carboxypeptidase E is necessary for its function as a regulated secretory pathway sorting receptor. J Biol Chem. 2000; 275:29887-29893.

18. Morris DG, Musat M, Czirjak S, Hanzely Z, Lillington DM, Korbonits M, Grossman AB. Differential gene expression in pituitary adenomas by oligonucleotide array analysis. Eur J Endocrinol. 2005; 153:143-151.
19. Armento A, Ilina EI, Kaoma T, Muller A, Vallar L, Niclou SP, Kruger MA, Mittelbronn M, Naumann U. Carboxypeptidase E transmits its anti-migratory function in glioma cells via transcriptional regulation of cell architecture and motility regulating factors. Int J Oncol. 2017; 51:702-714.
20. Huang SF, Wu HD, Chen YT, Murthy SR, Chiu YT, Chang Y, Chang IC, Yang X, Loh YP. Carboxypeptidase E is a prediction marker for tumor recurrence in early-stage hepatocellular carcinoma. Tumour Biol. 2016; 37:9745-9753.
21. Liu A, Shao C, Jin G, Liu R, Hao J, Shao Z, Liu Q, Hu X. Downregulation of CPE regulates cell proliferation and chemosensitivity in pancreatic cancer. Tumour Biol. 2014; 35:12459-12465.
22. Shen HW, Tan JF, Shang JH, Hou MZ, Liu J, He L, Yao SZ, He SY. CPE overexpression is correlated with pelvic lymph node metastasis and poor prognosis in patients with early-stage cervical cancer. Arch Gynecol Obstet. 2016; 294:333-342.
23. Wang ZQ, Faddaoui A, Bachvarova M, Plante M, Gregoire J, Renaud MC, Sebastianelli A, Guillemette C, Gobeil S, Macdonald E, et al. BCAT1 expression associates with ovarian cancer progression: possible implications in altered disease metabolism. Oncotarget. 2015; 6:31522-31543.
24. Fan S, Li X, Li L, Wang L, Du Z, Yang Y, Zhao J, Li Y. Silencing of carboxypeptidase E inhibits cell proliferation, tumorigenicity, and metastasis of osteosarcoma cells. Onco Targets Ther. 2016; 9:2795-2803.
25. Liang XH, Li LL, Wu GG, Xie YC, Zhang GX, Chen W, Yang HF, Liu QL, Li WH, He WG, et al. Upregulation of CPE promotes cell proliferation and tumorigenicity in colorectal cancer. BMC Cancer. 2013; 13:412.
26. Murthy SRK, Dupart E, Al-Sweel N, Chen A, Cawley NX, Loh YP. Carboxypeptidase E promotes cancer cell survival, but inhibits migration and invasion. Cancer Lett. 2013; 341:204-213.
27. Hareendran S, Yang X, Lou H, Xiao L, Loh YP. Carboxypeptidase E-N Promotes Proliferation and Invasion of Pancreatic Cancer Cells via Upregulation of CXCR2 Gene Expression. Int J Mol Sci. 2019; 20.
28. Yang X, Lou H, Chen YT, Huang SF, Loh YP. A novel 40kDa N-terminal truncated carboxypeptidase E splice variant: cloning, cDNA sequence analysis and role in regulation of metastatic genes in human cancers. Genes Cancer. 2019; 10:160-170.
29. Li Z, Ma YY, Wang J, Zeng XF, Li R, Kang W, Hao XK. Exosomal microRNA-141 is upregulated in the serum of prostate cancer patients. Onco Targets Ther. 2016; 9:139-148.
30. Logozzi M, De Milito A, Lugini L, Borghi M, Calabro L, Spada M, Perdicchio M, Marino ML, Federici C, Iessi E, et al. High levels of exosomes expressing CD63 and caveolin-1 in plasma of melanoma patients. PLoS One. 2009; 4:e5219.
31. Nilsson J, Skog J, Nordstrand A, Baranov V, Mincheva-Nilsson L, Breakefield XO, Widmark A. Prostate cancer-derived urine exosomes: a novel approach to biomarkers for prostate cancer. Br J Cancer.

2009; 100:1603-1607.

32. Skog J, Wurdinger T, van Rijn S, Meijer DH, Gainche L, Sena-Esteves M, Curry WT, Jr., Carter BS, Krichevsky AM, Breakefield XO. Glioblastoma microvesicles transport RNA and proteins that promote tumour growth and provide diagnostic biomarkers. Nat Cell Biol. 2008; 10:1470-1476.
33. Tanaka Y, Kamohara H, Kinoshita K, Kurashige J, Ishimoto T, Iwatsuki M, Watanabe M, Baba H. Clinical impact of serum exosomal microRNA-21 as a clinical biomarker in human esophageal squamous cell carcinoma. Cancer. 2013; 119:1159-1167.
34. Fan S, Gao X, Chen P, Li X. Carboxypeptidase E-DeltaN promotes migration, invasiveness, and epithelial-mesenchymal transition of human osteosarcoma cells via the Wnt-beta-catenin pathway. Biochem Cell Biol. 2019; 97:446-453.
35. Zomer A, Maynard C, Verweij FJ, Kamermans A, Schafer R, Beerling E, Schiffelers RM, de Wit E, Berenguer J, Ellenbroek SIJ, et al. In Vivo imaging reveals extracellular vesicle-mediated phenocopying of metastatic behavior. Cell. 2015; 161:1046-1057.
36. Alvarez-Erviti L, Seow Y, Yin H, Betts C, Lakhal S, Wood MJ. Delivery of siRNA to the mouse brain by systemic injection of targeted exosomes. Nat Biotechnol. 2011; 29:341-345.
37. Diehl JA. Cycling to cancer with cyclin D1. Cancer Biol Ther. 2002; 1:226-231.
38. Shintani M, Okazaki A, Masuda T, Kawada M, Ishizuka M, Doki Y, Weinstein IB, Imoto M. Overexpression of cyclin DI contributes to malignant properties of esophageal tumor cells by increasing VEGF production and decreasing Fas expression. Anticancer Res. 2002; 22:639-647.
39. Zheng K, Cubero FJ, Nevzorova YA. c-MYC-Making Liver Sick: Role of c-MYC in Hepatic Cell Function, Homeostasis and Disease. Genes (Basel). 2017; 8.
40. Akita H, Marquardt JU, Durkin ME, Kitade M, Seo D, Conner EA, Andersen JB, Factor VM, Thorgeirsson SS. MYC activates stem-like cell potential in hepatocarcinoma by a p53-dependent mechanism. Cancer Res. 2014; 74:5903-5913.

Figures

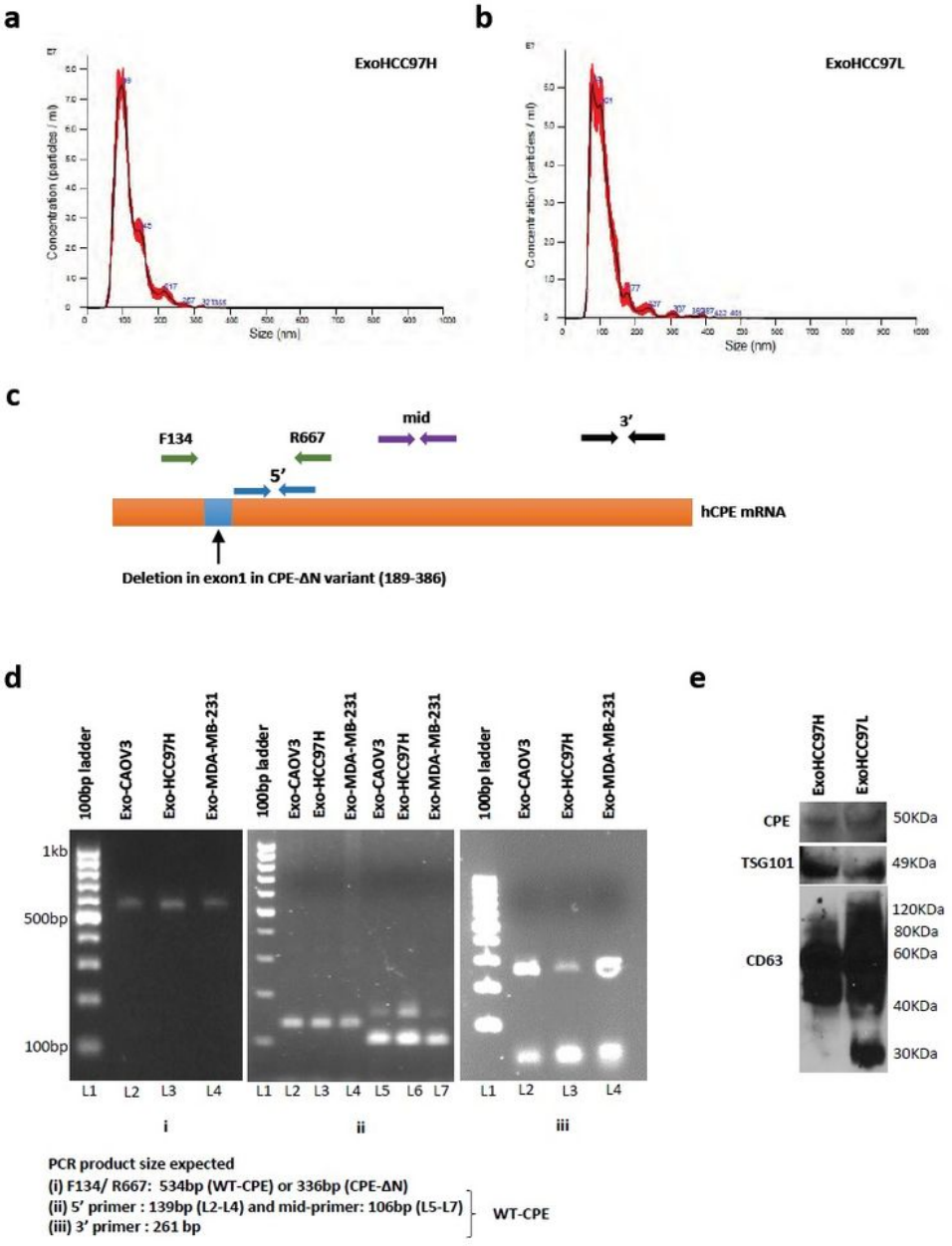

Figure 1

Detection of CPE in cancer cell exosomes. a-b Characterization of metastatic liver cancer cell derived exosomes: Representative graph (left panel) showing the concentration plotted against particle size of exosomes released from HCC97H (a) and HCC97L (b) cells, determined using NanoSight analysis. c Schematic showing human CPE mRNA with the position of RT-PCR primers used to detect CPE gene fragments. The region of deletion seen in exon 1 of CPE-ΔN variant, another isoform of CPE detected in

cancer cells is marked as a blue box and the F134/ R667 primer set used to distinguish WT-CPE and CPE-ΔN sequences are denoted by green arrows. d Exosomes isolated from CAOV3, HCC97H and MDA-MB-231 cells were analyzed using RT-PCR to determine the presence of CPE transcripts. Images of agarose gels showing the amplicons generated using the primers specific for 5'-end, middle or 3'-end parts of CPE mRNA, besides the region flanking the exon 1 deletion in CPE-ΔN sequence. The expected PCR product sizes are given below the gel images. Major band sizes represented by the 100bp DNA ladder are shown in d(i). e Western blot showing WT-CPE and exosomal markers TSG101 and CD63 in exosomes released from HCC97H and HCC97L cells. Full-length blots are presented in additional file 1: Fig. S2.

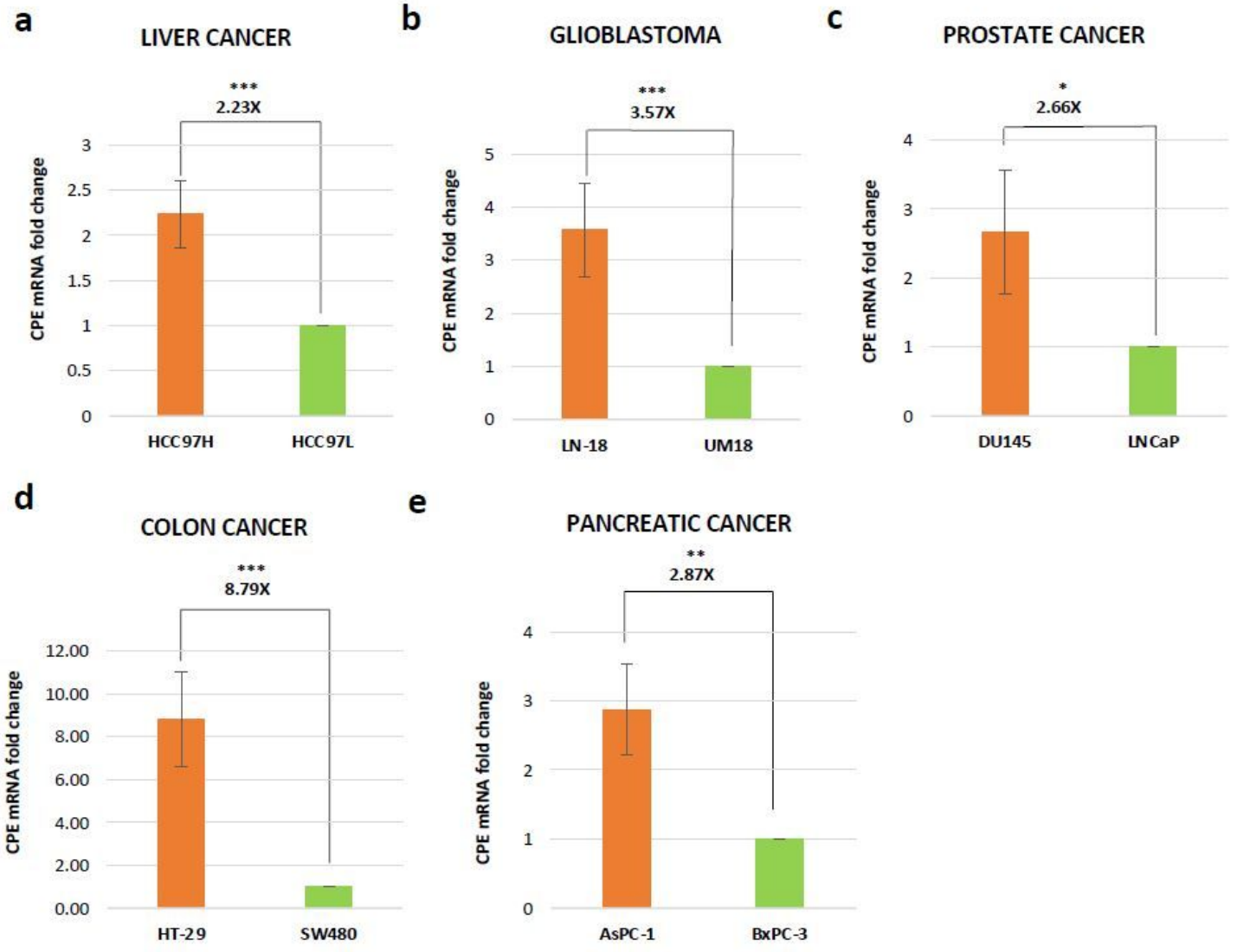

Figure 2

Highly malignant cancer cells release exosomes with elevated CPE copy numbers. a-e Bar graph showing the fold change of CPE mRNA copy numbers measured in exosomes derived from highly malignant/ aggressive cells (orange bars) versus low-malignant cells (green bars) from different types of cancer as

denoted in the figure (N=3 for b, c, e and N=2 for a, d). Error bars denote SE (b, c, e) and SD (a, d). Student's t-test: *, P < 0.05; **, P < 0.01; ***, P < 0.001.

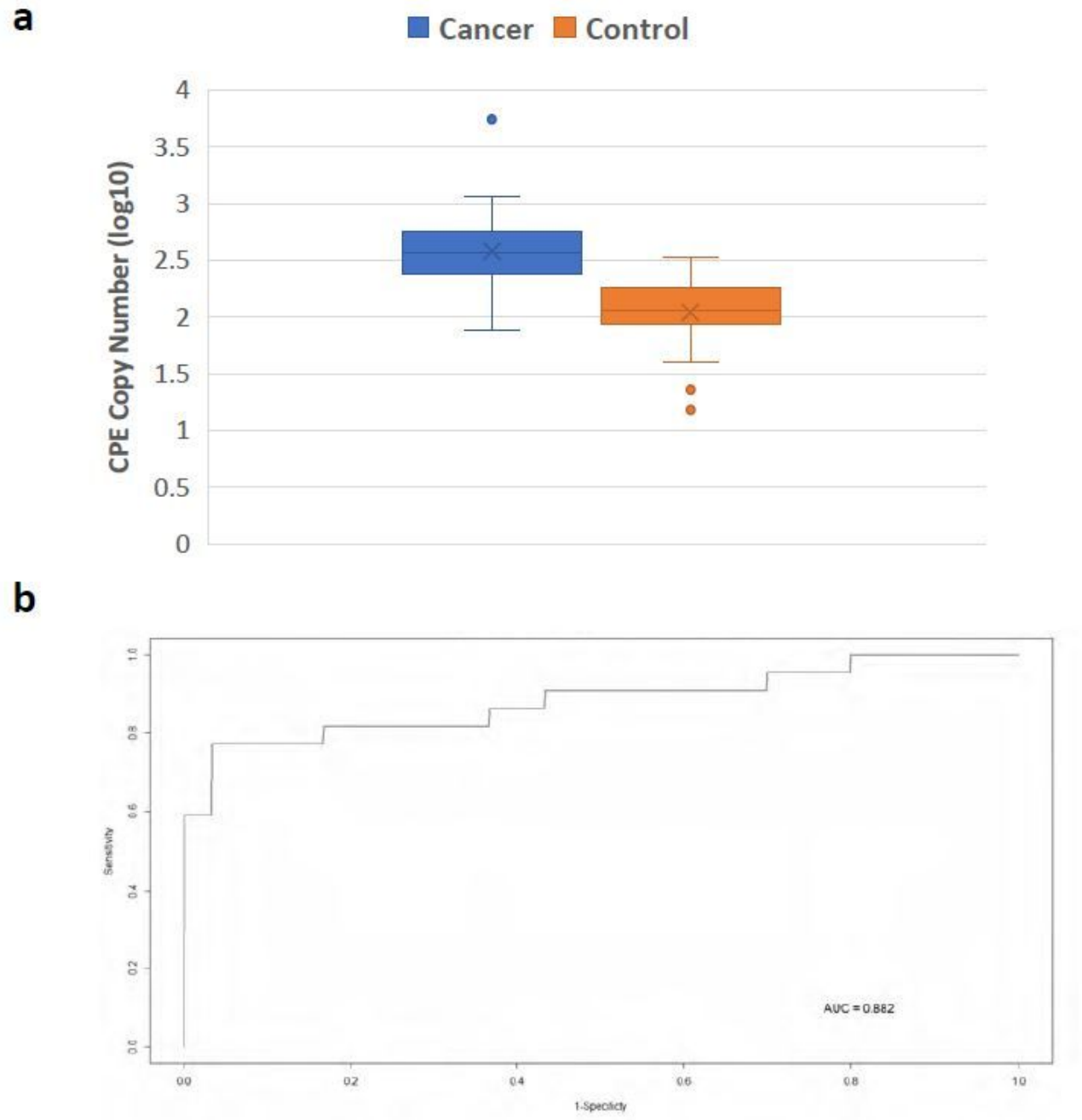

Figure 3

Serum exosomes from cancer patients are enriched in CPE mRNA. a Box plot showing the log-transformed data of CPE copy numbers in sera exosomes derived from cancer patients versus healthy subjects (p<0.001). b ROC curve of CPE copy numbers in exosomes from cancer patients' sera compared to control sera, showing the AUC. Types of cancer included (in cases) : Breast cancer (n=6), Ovarian cancer (n=5), Glioma (n=5), Colon cancer (n=2), Cervical cancer (n=1), Kidney cancer (n=1), Pancreatic cancer (n=1) and Prostate cancer (n=1).

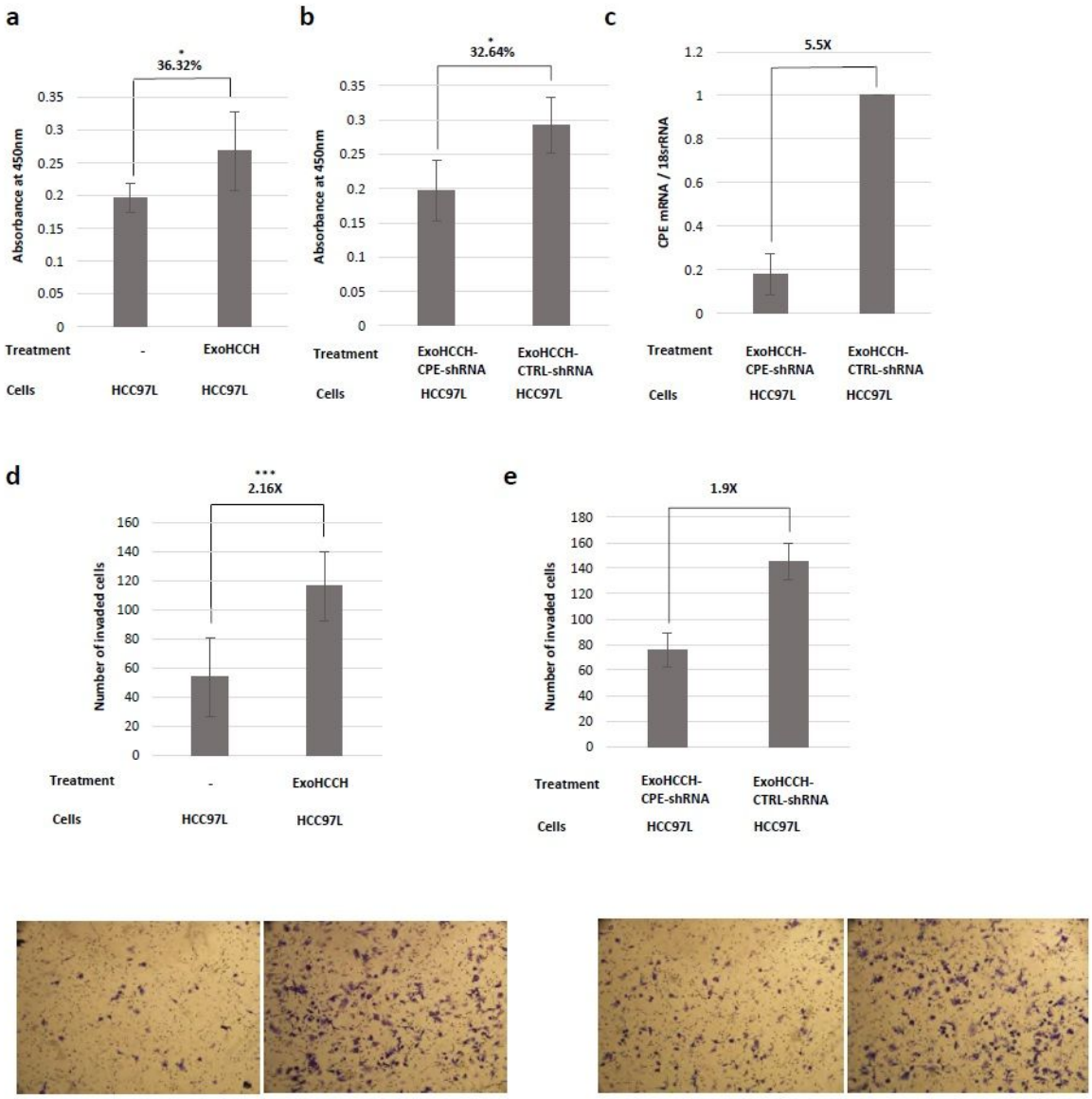

Figure 4

Exosomes from HCC97H cells enhance proliferation and invasion of recipient HCC97L cells in a CPE-dependent manner. a-b Bar graph showing the absorbance values obtained in the MTT cell proliferation assay on day 5 of HCC97L cells treated with exosomes from HCC97H cells (ExoHCCH, a) or with exosomes isolated after transfection of HCC97H cells with either CPE targeting shRNA or control shRNA, (ExoHCCH-CPE-shRNA/ExoHCCH-CTRL-shRNA, b) (N=2, n=3). ExoHCCH increase the proliferation of HCC97L cells, however down-regulation of CPE expression in HCC97H cells before exosome isolation abolishes this effect. c Bar graph showing the fold change in knockdown of CPE mRNA levels in HCC97L

cells treated with ExoHCCH-CPE-shRNA relative to cells treated with ExoHCCH-CTRL-shRNA (N=2). d-e Bar graph and representative images of wells showing the number of HCC97L cells that invaded through matrigel after treatment with ExoHCCH (d) (N=2, n=3), or with either ExoHCCH-CPE-shRNA or ExoHCCH-CTRL-shRNA (e) (N=1, n=3). HCCH97L cells treated with ExoHCCH exhibit enhanced invasion, and this effect is abolished if HCC97H cells are transfected with CPE-shRNA before exosome isolation. Error bars denote SD. Student's t-test: * ,P < 0.05; ***, P < 0.001.

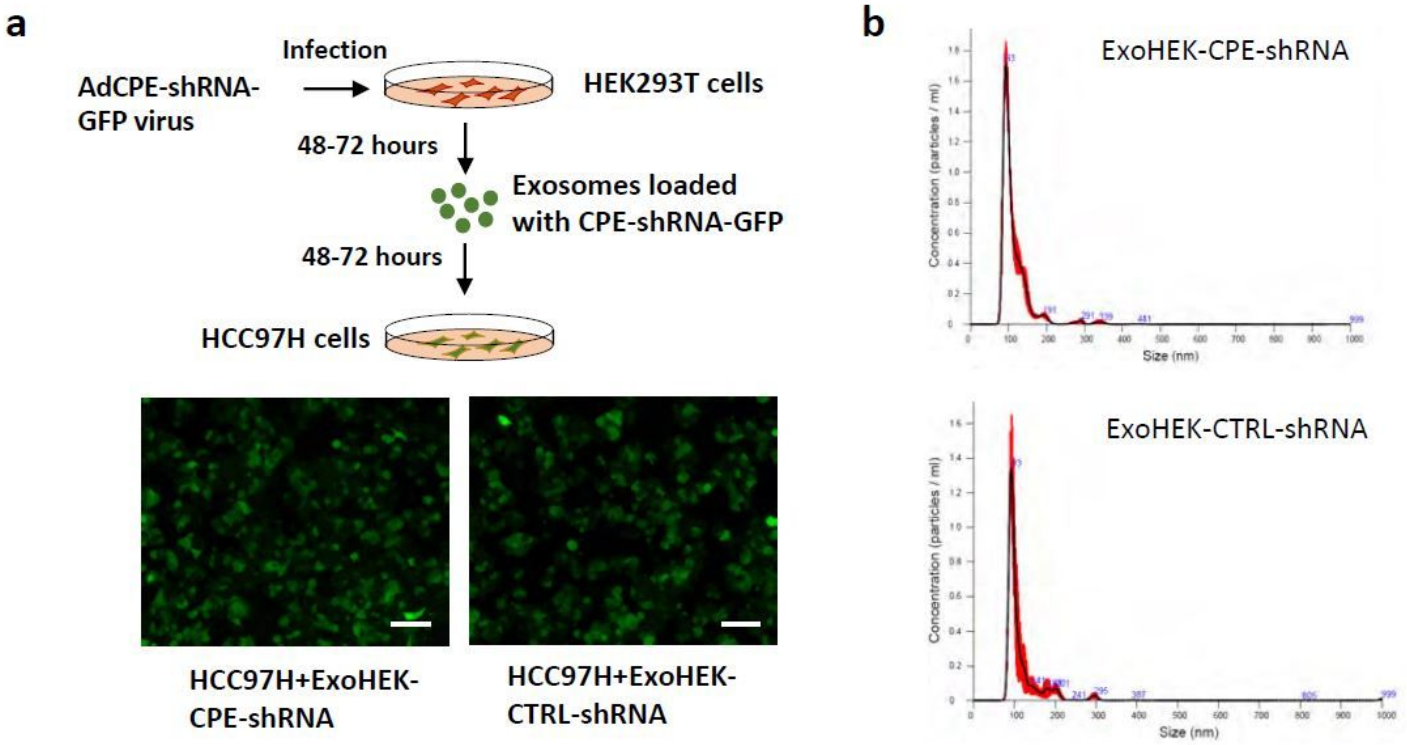

Figure 5

Characterization of exosomes loaded with CPE-shRNA. a Schematic showing the strategy of loading and transfer of CPE-shRNA via exosomes. Exosomes were isolated from supernatant media of HEK293T cells (ExoHEK) infected with adenovirus encoding either CPE-shRNA or CTRL-shRNA, fused to GFP. HCC97H cells treated with these modified exosomes exhibited green fluorescence, validating the transfer of CPE-shRNA through the exosomes. Representative images showing GFP fluorescence in target HCC97H cells, treated with either ExoHEK-CPE-shRNA or ExoHEK-CTRL-shRNA are included. Scale bar=100μm. b Graph showing the concentration and size distribution of ExoHEK-CPE-shRNA and ExoHEK-CTRL-shRNA, as determined by NanoSight analysis.

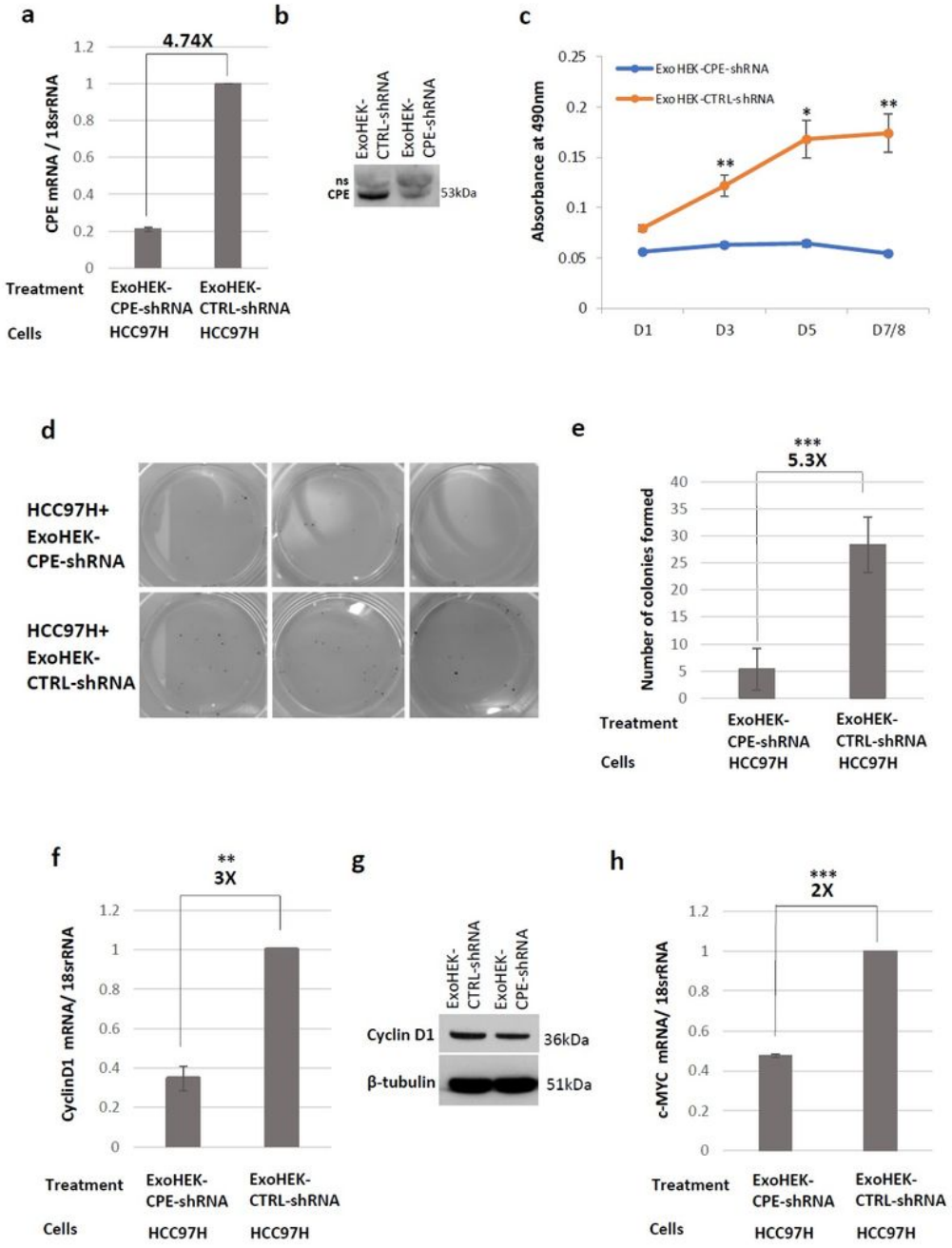

Figure 6

CPE-shRNA loaded exosomes inhibit proliferation of highly malignant HCC cells. a Bar graph showing the fold change in down-regulation of CPE mRNA levels in HCC97H cells treated with ExoHEK-CPE-shRNA in comparison to cells treated with ExoHEK-CTRL-shRNA (N=2). b Western blot showing suppressed secreted CPE levels (70.91% ±0.003 decrease) in the media of HCC97H cells treated with ExoHEK-CPE-shRNA relative to the media of cells treated with ExoHEK-CTRL-shRNA (N=2). ns: non-specific. c

Representative line graph showing the absorbance values obtained in the MTT cell proliferation assay from D1- D7/8 of HCC97H cells treated with HEK293T exosomes loaded with either CPE-shRNA or Control shRNA. CPE-shRNA loaded exosomes inhibit the proliferation of HCC97H cells (N=3, n=3). d-e Representative images and bar graph showing the number of colonies formed by HCC97H cells treated with ExoHEK-CPE-shRNA or ExoHEK-CTRL shRNA. Exosomes loaded with CPE-shRNA significantly decreased the colony formation ability of HCC97H cells (N=2, n=3). f Bar graph showing the down-regulation of Cyclin D1 mRNA expression in HCC97H cells incubated with ExoHEK-CPE-shRNA compared to the control (N=3). g Representative western blot showing reduced levels of Cyclin D1 (23.17% ±0.022 decrease) in HCC97H cells treated with ExoHEK-CPE-shRNA compared to cells treated with ExoHEK-CTRL-shRNA (N=2). Full-length blots are presented in additional file 1: Fig. S4. h Bar graph showing the suppression of c-MYC mRNA levels in HCC97H cells after treating with ExoHEK-CPE-shRNA relative to cells treated with ExoHEK-CTRL-shRNA (N=3). Error bars denote SD (a, c and e) and SE (f and h). Student's t-test: **, $P < 0.01$, ***, $P < 0.001$

Supplementary Files

This is a list of supplementary files associated with this preprint. Click to download.

- Supplfig022421.pdf
- Supplfile022421.docx
- GA.jpg